

Nanotomography endstation at the P05 beamline: Status and perspectives

This content has been downloaded from IOPscience. Please scroll down to see the full text.

2017 J. Phys.: Conf. Ser. 849 012056

(<http://iopscience.iop.org/1742-6596/849/1/012056>)

View [the table of contents for this issue](#), or go to the [journal homepage](#) for more

Download details:

IP Address: 129.13.72.197

This content was downloaded on 26/07/2017 at 15:53

Please note that [terms and conditions apply](#).

You may also be interested in:

[String Theory and the Real World: Perspectives](#)

G Kane

[The nanotomography endstation at the PETRA III Imaging Beamline](#)

M Ogurreck, F Wilde, J Herzen et al.

[Scanning Transmission X-ray Microscopy with X-ray Fluorescence Detection at the XUV Beamline P04, PETRA III, DESY](#)

K Andrianov, L Lühl, T Nisius et al.

[Merkel opens PETRA III hall](#)

[Nanodiffraction at MINAXS \(P03\) beamline of PETRA III](#)

C Krywka, J Keckes, S Storm et al.

[Addendum: The hard X-ray Photon Single-Shot Spectrometer of SwissFEL—initial characterization](#)

J. Rehanek, M. Makita, P. Wiegand et al.

[Induced Absorption in X-ray-Irradiated CdS-Doped Glass](#)

Tadaki Miyoshi, Keita Ushigusa, Masakatsu Tamechika et al.

[Time-resolved soft X-ray microscopy of magnetic nanostructures at the P04 beamline at PETRA III](#)

P Wessels, J Ewald, M Wieland et al.

[The BALDER Beamline at the MAX IV Laboratory](#)

K Klementiev, K Norén, S Carlson et al.

Nanotomography endstation at the P05 beamline: Status and perspectives

I Greving¹, M Ogurreck^{1,4}, F Marschall², A Last³, F Wilde¹, T Dose¹, H Burmester¹,
L Lottermoser¹, M Müller¹, C David² and F Beckmann¹

¹Helmholtz-Zentrum Geesthacht, Institute of Materials Research, Germany

²Paul Scherrer Institut, Laboratory for Micro- and Nanotechnology, PSI, Switzerland

³Karlsruhe Institute of Technology, Institute of Microstructure Technology, Germany

⁴Diamond Light Source Ltd, Didcot, UK

imke.greving@hzg.de

Abstract. The Imaging Beamline IBL/P05 at the DESY storage ring PETRA III, operated by the Helmholtz-Zentrum Geesthacht, has two dedicated endstations optimized for micro- and nanotomography experiments [1-3]. Here we present the status of the nanotomography endstation, highlight the latest instrumentation upgrades and present first experimental results. In particular in materials science, where structures with ceramics or metallic materials are of interest, X-ray energies of 15 keV and above are required even for sample sizes of several 10 μm in diameter. The P05 imaging beamline is dedicated to materials science and is designed to allow for imaging applications with X-ray energies of 10 to 50 keV. In addition to the full field X-ray microscopy setup, the layout of the nanotomography endstation allows switching to cone-beam configuration. Kinematics for X-ray optics like compound refractive lenses (CRLs), Fresnel zone plates (FZP) or beam-shaping optics are implemented and the installation of a Kirkpatrick Baez-mirror (KB mirror) system is foreseen at a later stage of the beamline development. Altogether this leads to a high flexibility of the nanotomography setup such that the instrument can be tailored to the specific experimental requirements of a range of sample systems.

1. Introduction

X-ray imaging is a vital tool to study the structure of materials for a wide range of sciences e.g. medicine, biology, archaeology and geology [1,7,8]. Also for engineering materials this technique is important, allowing for a better knowledge of the inner structure, the material porosity or crack propagation, helping to understand failure mechanisms and thus optimizing the production process. Standard micro CT routinely allows resolutions down to about 1 μm .

A range of scientific questions however, require a higher spatial resolution in order to resolve structures in the nanometer range. Scanning electron microscopy allows imaging in this size regime, but is limited to surface analysis. Transmission electron microscopy (TEM) however requires very thin samples of a few hundred nanometres in thickness and only gives very limited information about the bulk structure of a material. Focused Ion Beam (FIB) tomography on the other hand can offer resolutions of better than 5 nm [8] and offers 3D information. Issues like curtaining effects and long-term stability however limit this technique to sample diameters of below 10 μm . In addition no in situ measurements of the sample can be performed and the sample is destroyed during the layer – by – layer decomposition.

X-ray microscopy in contrast is a non-destructive method to acquire 3D information of the bulk sample with resolutions down to below 50 nm in the hard X-ray regime. In addition, the high flux at synchrotron sources enables good time resolution and the high coherence opens up a range of phase contrast methods for x-ray microscopy or holotomography for cone – beam setups. Choosing the right set of optics, also sample environments can be used for in situ investigations at the nanometer scale.



Here we present the status and perspectives of the nanotomography setup at the P05 / Imaging Beamline IBL operated by the Helmholtz Zentrum Geesthacht (HZG) at PETRA III storage ring at DESY in Hamburg (Germany).

2. Experimental Setup

2.1. Layout of the Imaging Beamline IBL / P05

The beamline is dedicated to materials science and allows visualizing structural properties in the range of several micrometers down to the nanometer regime [1-4]. It comprises of two experimental stations: A micro – and a nanotomography station, a sketch of the beamline is given in figure 1 (left). The optics hutch of the IBL beamline is equipped with two monochromators: A Double Crystal Monochromator (DCM) and a Double Multilayer Monochromator (DMM) both allowing for an energy range of 5 – 50 keV. The DCM has an energy bandwidth of $\Delta E/E \sim 10^{-4}$ while the installed DMM which is currently under commissioning, will allow for higher flux at an energy bandwidth of $\Delta E/E \sim 10^{-2}$ with multilayer coatings produced inhouse by HZG [5].

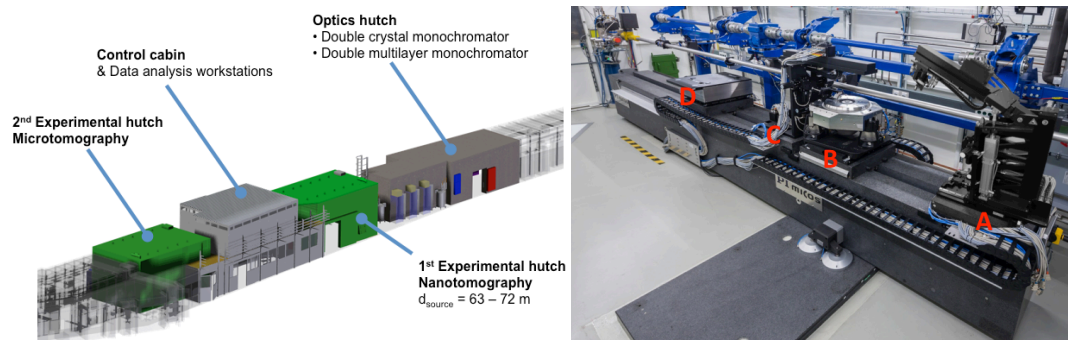


Figure 1. Left: Beamline IBL/P05 overview [2]. Right: Photograph of the experimental hutch with two optics stations and high precision sample rotation stage in between. The four granite slabs can move independently from each other. On the 4th slab a detector system can be mounted.

2.2. Nano Tomography Endstation

The nanotomography endstation shown in figure 1 (right) is a highly flexible setup [1-3] dedicated to full field nano imaging. On top of the 6.8 m long granite substructure four granite slabs are mounted on air bearings and can be moved independently. On the first slab, closest to the source (right hand side in figure 1, A) a six – axis optics kinematics stage is mounted and the extension arm is fitted with high precision apertures. This extension arm can be moved in and out of the beam path e.g. for switching between X – ray microscopy and cone beam geometry. The second slider (B in figure 1, right) holds the sample stage, consisting of a high precision rotation stage and a linear axis to move the sample perpendicular to the incoming beam. The air – bearing rotation stage itself is mounted on three pods allowing for height as well as tip/tilt alignment of the sample stage. Overall a wobble and axial error of less than 30 nm (RMS) is achieved for the sample rotation. The sample itself is mounted on a six – axis kinematics in the center of the rotation stage allowing for precise alignment of the sample in the center of rotation. On the third slider (C in figure 1, right) a second optics station is installed, mirroring the stage on the first slider (A). It is also equipped with a six – axis kinematics and a set of high precision apertures (e.g. used as order selecting apertures for X – ray microscopy using FZP). The extension arm can be varied in length depending on the requirements of the experiment. For precise alignment of the X – ray optics a second camera system (PixeLink) is installed at 300 mm behind the optics stage on the third slider (C in figure 1, right). This alignment camera can be moved remotely in and out of the beam path and is equipped with a 100 μm thick CdWO_4 scintillator crystal and yields a 10x light optical magnification, thus achieving an effective pixel size of $\sim 0.6 \mu\text{m}$. The detector system for the tomography setup is mounted on the last slider (D in figure 1, right).

Currently a pco.edge 4.2 is installed with a LuAG scintillator of $30\ \mu\text{m}$ thickness. The sCMOS chip is cooled to $0\ ^\circ\text{C}$, consists of 2048×2048 pixels with a pixel size of $6.4\ \mu\text{m}$. Different magnifications of the visible light optics can be chosen $M=7-12$, yielding effective pixel sizes between $0.54\ \mu\text{m}$ and $0.92\ \mu\text{m}$ with an numerical aperture of 0.34.

3. Experimental Results

An X-ray microscope for different energies has been installed at the nanotomography endstation. Two different sets of optics were chosen depending on energy: For the lower energy regime ($< 15\text{ keV}$) a Fresnel zone plate (FZP) was installed as an objective lens and a diffractive beamshaper as condenser optics, both manufactured at the PSI. The design energy for the FZP is $14\ \text{keV}$ with an outermost zone width of $80\ \text{nm}$ and a working distance of $70\ \text{mm}$. The fields of the beamshaper are $50\ \mu\text{m} \times 50\ \mu\text{m}$ in size, covering a field of $1.8\ \text{mm} \times 1.8\ \text{mm}$. For the higher energy regime ($>15\ \text{keV}$) polymer compound refractive lenses (CRLs) were used as objective lenses and a rolled prism lens as condenser optics [6,9]. The optics were fabricated at the Institute of Microstructure Technology (IMT) at the Karlsruhe Institute of Technology in Karlsruhe (KIT) using X-ray lithography. These CRLs allow for resolving line widths below $100\ \text{nm}$ and the VHVHV – design of alternating vertical and horizontal lens elements ensures minimal astigmatism [6]. The working distance of these lenses is around $100\ \text{mm}$.

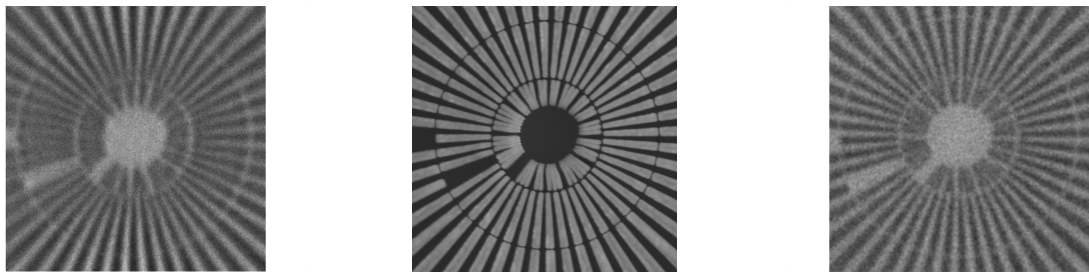


Figure 2. XRM images of Xradia test pattern. Inner circle $50-100\ \text{nm}$ lines, 2nd circle $100-200\ \text{nm}$ lines: Left: using CRL setup at $17.4\ \text{keV}$ and a rolled prism lens as a condenser; Right: using FZP setup at $14\ \text{keV}$ with a mosaic lens as condenser optics. Middle: SEM image of the test pattern, revealing that the $50\ \text{nm}$ structures in the center are collapsed.

Performing a resolution test using an Xradia test pattern shows that with both setups the $100\ \text{nm}$ lines of the Siemens star are well resolved (Figure 2). It has to be noted, that the image from the CRL setup was acquired with a pco.4000 CCD camera combined with an LSO scintillator with a thickness of $16\ \mu\text{m}$. For the FZP setup the pco.edge 4.2 was used (see section 2.2) in combination with the $30\ \mu\text{m}$ LuAg scintillator. The reconstructed data shown in figure 3 have been acquired using the FZP setup at $14\ \text{keV}$. The nano porous gold sample was prepared by Focused Ion Beam (FIB) and the sample cross-section is $8\ \mu\text{m} \times 8\ \mu\text{m}$. The SEM image of the sample reveals the nano structure, which is also clearly visible in the reconstructed volume shown in figure 3 on the right hand side. The gold filaments are in the order of $400\ \text{nm}$ in width and are clearly resolved in the three dimensional image.

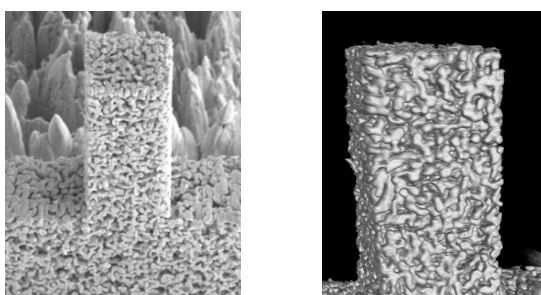


Figure 3. Nano porous gold. Left: SEM image; Right: Rendering of reconstructed volume. The experiment was performed using the FZP setup at an energy of $14\ \text{keV}$ (eff. pixel size $17.4\ \text{nm}$). The square column has an edge length of about $8\ \mu\text{m} \times 8\ \mu\text{m}$ and was prepared by FIB milling. The filament sizes of the NPG sample are in the range of $400\ \text{nm}$ in width and are nicely resolved.

4. Future Perspectives

In the future better image statistics will be reached by implementing a new visible – light optics design with a higher numerical aperture. This new camera system will house up to three cameras permanently mounted and aligned with respect to the sample stage. A movable mirror will allow for switching in between the different cameras. This way the alignment of the experimental setup and the optics can be done using a fast camera, e.g. a scientific CMOS and the tomography will then be performed using a CCD with high statistics. Another increase in image quality and decrease in scan time will be reached by using the newly installed DMM, once it is fully commissioned.

Furthermore it is planned to commission a cone beam setup and make it available to users. In contrast to X-ray microscopy geometry the cone beam technique offers a higher flexibility, e.g. the FoV depends on the chosen sample to detector distance and not on the chosen objective lens. The technique also allows for the implementation of sample environments, since in X-ray microscopy setups the space around the sample is often very limited. A specifically designed in vacuum six-axis kinematics is installed in the vacuum tank in the optics hutch such that a pre – focusing device can be implemented there. In order to align these pre – focusing optics an additional camera system equipped with a scintillator will also be installed in the vacuum tank and is currently in the design state. This in combination with the DMM will offer a very flexible cone beam setup at the instrument in the future.

Acknowledgements

The authors thank Prof. E. Lilleodden and her group (HZG, Institute of Materials Mechanics) for the nanoporous gold sample imaged at P05 (figure 3). I. G. acknowledges the Virtual Institute of New X-ray Analytic Methods in Material Science (VI – NXMM) for funding. M. O. gratefully acknowledges financial support from the German Research Foundation (DFG) via SFB 986 M3, project Z2. The authors thank Harald Vogt of the Karlsruhe Institute for Microstrukturertechnology (IMT) and the Karlsruhe Nano Micro Facility (KNMF) for the design and fabrication of the rolled X-ray prism lenses.

References

- [1] Greving I, Wilde F, Ogurreck M, Herzen J, Hammel J U, Hipp A, Friedrich F, Lottermoser L, Dose T, Burmester H, Müller M and Beckmann F. Proc. SPIE 9212, Developments in X-Ray Tomography IX, 92120O-8, 2014
- [2] Ogurreck M, Wilde F, Herzen J, Beckmann F, Nazmov V, Mohr J, Haibel A, Müller M, and Schreyer A, Journal of Physics: Conference Series, vol. 425, p. 182002, 2013
- [3] Wilde F, Ogurreck M, Greving I, Hammel J U, Beckmann F, Hipp A, Lottermoser L, Khokhriakov I, Lyatev P, Dose T, Burmester H, Müller M, and Schreyer A, AIP Conference Proceedings 1741, 030035, 2016
- [4] Ogurreck M, do Rosario J J, Leib E W, Laipple D, Greving I, Marschall F, Last A, Schneider G A, Vossmeier T, Weller H, J. Synchrotron Rad. 23, 2016
- [5] Störmer M, Horstmann C, Häussler O, Spiecker E, Siewert F, Scholze F, Hertlein F, Jäger W, and Bormann R, SPIE, vol. 7077, p. 707705, 2008.
- [6] Marschall F, Last A, Simon M, Kluge M, Nazmov V, Vogt H, Ogurreck M, Greving I, and Mohr J, Journal of Physics: Conference Series, vol. 499, p. 012007, 2014
- [7] Sakdinawat A and Attwood D, Nature photonics, vol. 4, p 840 – 848, 2010
- [8] Möbus G, Inkson B J, Materials Today, vol.10, p 18-25, 2015
- [9] Reznikova E, Weitkamp T, Nazmov V, Last A, Simon M, Saile V, Physica Status Solidi, p 2811-2816, vol. 204, 2007